Appl. Phys. B 69, 291–301 (1999) / Digital Object Identifier (DOI) 10.1007/s003409900128

Applied Physics B
Lasers
and Optics

A neutral atom and a wire: towards mesoscopic atom optics

J. Denschlag[1], **D. Cassettari**[1,2], **A. Chenet**[1], **S. Schneider**[1], **J. Schmiedmayer**[1]

[1] Institut für Experimentalphysik, Universität Innsbruck, A-6020 Innsbruck, Austria
[2] Dipartimento di Fisica - Universita' di Pisa, Piazza Torricelli 2, 56126 Pisa, Italy

Received: 13 December 1998/Revised version: 8 July 1999/Published online: 8 September 1999

Abstract. A large variety of trapping and guiding potentials can be designed by bringing cold atoms close to charged or current-carrying material objects. Using a current-carrying wire we demonstrate how to build guides and traps for neutral atoms and using a charged wire we study a $1/r^2$ singularity. The simplicity and versatility of the principles demonstrated in our experiments will allow for miniaturization and integration of atom optical elements into matter-wave quantum circuits.

PACS: 03.75.Be; 03.65.Nk

In electronics and light optics, miniaturization of components and integration into networks lead to new very powerful tools and devices, for example in quantum electronics [1] or integrated optics [2]. It is essential for the success of such designs that the size of the structures is, at least in one dimension, comparable to the wavelength of the guided wave. Similarly we anticipate that atom optics [3] if brought to the microscopic scale will give us a powerful tool to combine many atom optical elements into quantum matter wave networks.

Microscopic-scale atom optics can be realized by bringing cold atoms [4, 5] close to nanostructured material objects [6]. These cold atoms can have typical deBroglie wavelengths, λ_{dB} on the order of 100 nm or larger which is in the regime where one can easily design and build structures. In this paper we concentrate on two ways to construct microscopic potentials by using [6]: (i) the electric interaction between a neutral, polarizable atom and a charged nanostructure ($V_{\mathrm{el}} = -\frac{1}{2}\alpha E^2$), and (ii) the magnetic interaction between the atom's magnetic moment μ and a magnetic field B, $V_{\mathrm{mag}} = -\boldsymbol{\mu} \cdot \boldsymbol{B}$. In addition these potentials can be combined with traditional atom optical elements such as atom mirrors and evanescent light fields. A variety of novel atom optical elements for trapping and guiding can then be constructed at the microscopic scale like quantum wells, quantum wires, and quantum dots for neutral atoms. These elements can then further be combined to form more complex structures as, for example, coherent beamsplitters and registers for quantum computing.

In order to investigate these concepts experimentally we chose to work with thin, free-standing wires and cold lithium atoms. We present an overview of our experiments in recent years investigating the atomic interaction with thin charged [7, 8] wires and current-carrying wires [9–13] and discuss the implications of our experiments on the creation of mesoscopic atom optics [6], see Fig. 1. The paper is organized as follows:

In Sect. 1 we study a neutral atom interacting with the magnetic field of a current-carrying wire. Within this context we demonstrate two different atom guides: atoms are guided along the wire either circling in Kepler-like orbits around it or by moving inside a potential tube on the side of the wire.

In Sect. 2 we describe the interaction between a neutral polarizable atom and the electric field of a charged wire which allows the study of a $1/r^2$ singularity. By replacing the charged wire by a charged optical fiber still another atom guide can be constructed. The blue-detuned light propagat-

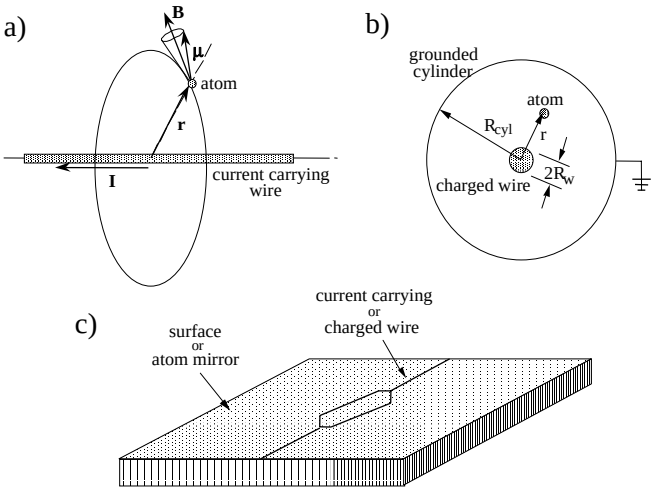

Fig. 1a–c. Schematics of neutral atoms interacting with a thin wire. **a** Interaction of a neutral atom (magnetic moment $\boldsymbol{\mu}$) with the magnetic field $\boldsymbol{B}$ of a wire carrying a current I. **b** A neutral atom and a charged wire. **c** Basic concept of constructing integrated atom optics by placing the wires on the surface or on an atomic mirror

ing in the fiber creates a short-range repulsive potential that prevents the guided atoms from hitting the fiber surface.

Section 3 discusses the design of microscopic guides and traps by mounting thin charged or current carrying wires on a surface. By combining different wires one can construct beam splitters, interferometers, or more complex matter-wave networks, creating mesoscopic atom optics.

1 An atom and a current

Neutral particles with a magnetic moment can be trapped using magnetic fields. A particle with total spin $\boldsymbol{F}$ and magnetic moment $\boldsymbol{\mu} = g_{\mathrm{F}}\mu_{\mathrm{B}}\boldsymbol{F}$ experiences the potential $V = -\boldsymbol{\mu}\cdot\boldsymbol{B}$. In general the vector coupling $\boldsymbol{\mu}\cdot\boldsymbol{B}$ results in a very complicated motion for the atom. However, in our experiments the Larmor precession (w_{L}) of the magnetic moment is much faster than the apparent change of direction of the magnetic field in the rest frame of the moving atom (w_{B}) and an adiabatic approximation can be applied. The magnetic moment then follows adiabatically the direction of the field and the atom can be described as moving in a scalar potential $V = -g_{\mathrm{F}}\mu_{\mathrm{B}}F_{\parallel}B$, where $F_{\parallel}$ is the projection of $\boldsymbol{F}$ on $\boldsymbol{B}$.

There are two possibilities to magnetically trap a particle with a magnetic moment μ, depending on the orientation of the magnetic moment relative to the direction of a static magnetic field.

(i) For the magnetic moment pointing in the same direction as the magnetic field (*strong-field-seeking* state), a minimum of the potential energy is found at a *maximum* of the field. Since the Earnshaw theorem forbids a local maximum of the magnetic field in free space [16, 17], a material source of the magnetic field has to be located inside the trapping region. This is often regarded as a disadvantage because trapped atoms may hit the material object. A possible realization of such a trap is a current-carrying wire [9–13, 18] with the atom orbiting around it (Fig. 2a) as discussed in Sect. 1.2.

(ii) For the magnetic moment pointing in the opposite direction of the magnetic field (*weak-field-seeking* state) particles are trapped in a *minimum* of the magnetic field. Because a minimum of the magnetic field in free space is not forbidden by the Earnshaw theorem, weak-field-seeking traps are most common for trapping neutral atoms. In Sect. 1.3 we describe how to design potentials for guiding and trapping of low-field-seekers by combining the magnetic field generated by a current-carrying wire with an external bias field [12, 13] (Fig. 2b).

1.1 Experiment

To study guides and traps created by a current-carrying wire we use laser-cooled lithium atoms from a magneto-optic trap (MOT) (see Fig. 3 and [12, 13]). The cold atoms are subjected to the guiding potentials in which their motion is studied. Our experiments are carried out in four steps (see Fig. 4):

1. First we load about 2×10^7 lithium atoms into a magneto-optic trap (MOT), displaced typically 1 mm from the wire to prevent trap losses due to atoms hitting the wire (see also Sect. 2.1 and [8]).
2. After loading the trap we shut off the slower beam and within 5–30 ms we shift the atoms to the position where they are loaded into the atom guide. This shifting is done by applying an additional magnetic offset field and moving the center of the magnetic quadrupole field, which defines the position of the MOT. Simultaneously the frequency and intensity of the trapping lasers are changed to control the size and temperature of the atom cloud (typically 1.6 mm diameter (FWHM) and $T \approx 200\,\mu$K which corresponds to a velocity of about 0.5 m/s).
3. We then release the atoms from the MOT by switching off the laser light, the MOT magnetic fields, and the shifting fields within 0.5 ms. At this point the current through the wire (typically 1 A) and, if desired, an additional bias magnetic field is switched on within 100 μs. From then

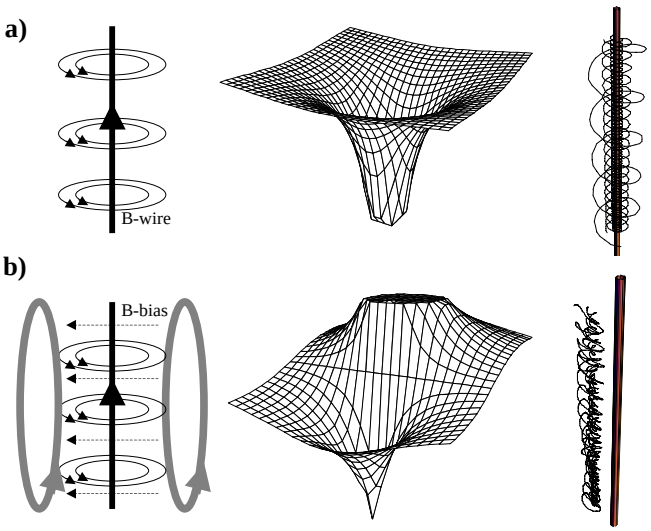

Fig. 2a,b. Guiding a neutral atom using a current-carrying wire. **a** Guiding the atoms in their *high-field-seeking* state as they circle around the wire. **b** Atoms can also be held in a 2-dimensional magnetic quadrupole field which is created by adding a constant bias field to the wire field

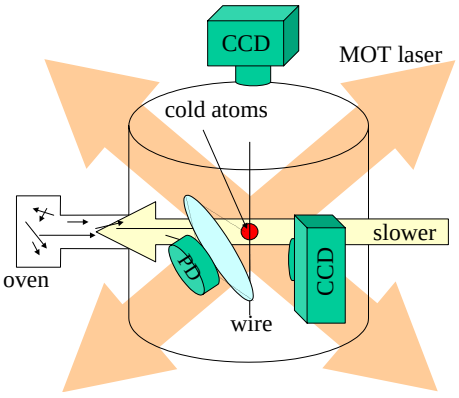

Fig. 3. Experimental setup for the wire experiments. The atoms are loaded into the MOT from an effusive thermal beam at a red laser detuning of 25 MHz and a total beam power of about 150 mW. To increase the loading rate by a factor of 5 an additional 20 mW slower beam is directed through the MOT into the oven. The atoms are observed with a photodiode and two triggerable standard CCD cameras (Pulnix TM670, 8 bit monochrome). They permit us to take pictures from above (looking along the wire) and from the side (looking onto the wire). In addition a lens images the cloud of the trapped atoms onto a photodiode that is used to measure the total atom number

on the atoms move in the tailored guiding potential. Starting from an initially well-localized atom cloud the density distribution expands and changes shape according to the forces acting on the atoms. Only those atoms that are in the correct spin state can be trapped and guided.

4. After a given guiding/trapping time, the spatial distribution of the atoms is measured by imaging the fluorescence from optical molasses [4] using two CCD cameras. (looking in wire direction and in direction orthogonal to the wire). This allows us to study both the radial confinement and the guiding of the atoms along the wire. For these measurements the guiding fields (current through the wire and bias field) are switched off and molasses laser beams are switched on for a short time (typically < 1 ms).

1.2 Interaction between an atom and a rectilinear current: the Kepler guide

Trapping a neutral particle with a magnetic moment in the magnetic field of a current-carrying wire was first proposed by Vladimirskii in 1961 [18] for the spin 1/2 neutron. It is a textbook example of an integrable system that is experimentally realizable as demonstrated in 1992 by guiding an effusive beam of thermal Na atoms (mean velocity ≈ 600 m/s) along a 1-m-long current-carrying wire [9].

The interaction potential of a neutral atom in the field of a rectilinear current I is given by:

$$V_{\mathrm{mag}} = -\boldsymbol{\mu}\cdot\boldsymbol{B} = -\frac{\mu_0 I}{2\pi}\frac{1}{r}\hat{e}_\varphi\cdot\boldsymbol{\mu}, \tag{1}$$

where $\hat{e}_\varphi$ is the circular unit vector in cylindrical coordinates. Using the adiabatic approximation V_{mag} corresponds to a two-dimensional Coulomb potential, $(1/r)$ in which atoms move in Kepler orbits[1] [19]. Typical parameters are given in Table 1.

In the quantum regime, the system looks like a two-dimensional hydrogen atom in (nearly circular) Rydberg states. The wire resembles the "nucleus" and the atom now takes the place of the "electron". Considerable theoretical work has been published on the quantum mechanical treatment of this system showing a hydrogen-like energy spectrum, [11, 20–23].

[1] By applying the adiabatic approximation [15], we obtain an effective Hamiltonian for the orbital motion of the atom where the Coulomb-like binding potential is corrected by a small repulsive $1/r^2$ interaction [11]. As a result, the adiabatic orbits are Kepler-like, and show an additional precession around the wire

Table 1. Typical parameters for alkali atoms trapped in circular orbits on a current-carrying wire. The upper part gives the values for the classical regime ($L \gg 100\hbar$), the lower part for the quantum regime ($L \leq 100\hbar$)

Atom	Current	r_{0rb} μm	Binding energy neV	L $\hbar$	ω_{0rb} rad/s	v_{0rb} cm/s
Li	2 A	100	120	$20\,10^3$	17800	178
Rb	2 A	100	120	$69\,10^3$	5096	51
Li	2.58 mA	2	7.4	100	226800	45
Rb	0.21 mA	2	0.6	100	18462	3.7

Experimental realization of Kepler guide. Using the experimental setup described in Sect. 1.1 we studied guiding of atoms while they circled around a current carrying wire (typical pictures are shown in Fig. 5). The atoms are released from the MOT at $t = 0$ in the center of a 10 cm long wire. A fraction of these atoms will be bound by the guiding potential, the rest forms an expanding cloud that quickly fades away within about 15 ms. The bound atoms are guided along the wire corresponding to their initial velocity component in this direction. Consequently, a cylindrical atomic cloud forms that expands along the wire. For long guiding times (we observed guiding up to 40 ms) the bound atoms leave the field of view, and the fluorescence signal of the atoms decreases. The top-view images of Fig. 5 show a round atom cloud that is centered on the wire suggesting that atoms circle around the wire.

The CCD pictures can be used for further analysis and detailed measurements. We can extract quantitative information about the spatial distribution and the number of atoms that are bound to the Kepler guide. Starting out with a sample of unpolarized atoms (200 μK and 1.6 mm FWHM diameter) we obtained a loading efficiency of about 10% for 1 A current through the wire, in very good agreement with Monte Carlo calculations. By optically pumping the atoms, and optimizing the trap size and current through the wire it should be possible to guide over 40% of the atoms in a thermal cloud with the Kepler guide. The loading efficiency is limited to this amount, because atoms in highly eccentric orbits will hit the wire and be lost.

We were also able to extract the momentum distribution of the guided atoms, by studying the ballistic expansion of the bound atoms after switching off the guiding potentials. Figure 6 shows a movie of how the atomic cloud expands as a function of time. Starting from a well-localized cylindrical cloud of guided atoms at $t = 0$ the spatial atomic distribution transforms into a doughnut-like shape. This is because in the Kepler guide, where atoms circle around the wire, there are no zero-velocity atoms. In other words, in order to be trapped in stable orbits *around* the wire the atoms need sufficient angular momentum and therefore velocity. Atoms with too little angular momentum hit the wire and are lost.

1.3 Guiding atoms on the side of the wire: the side guide

We now show that just by adding a constant bias field $\boldsymbol{B}_{\mathrm{b}}$ in a direction orthogonal to the wire (Fig. 2b) a another novel atom guide can be constructed. The bias field cancels exactly the circular magnetic field of the wire along a line parallel to the wire at a distance $r_s = (\mu_0/2\pi)(I/B_{\mathrm{b}})$. Around this line the modulus of the magnetic field increases in all directions and forms a tube with a magnetic field minimum in its center. Atoms in the weak-field-seeking state can be trapped in this two-dimensional quadrupole field and guided along the side of the wire. In this configuration trapped atoms can be lost by Majorana transitions between the trapped and untrapped spin states when they cross the central zero-field line. However, this problem can be circumvented by adding a small B-field component along the wire direction. This illustrates that by choosing appropriate magnetic bias fields the guiding potential and its characteristics can be tailored at will. The deeper reason for this freedom in creating a whole variety of

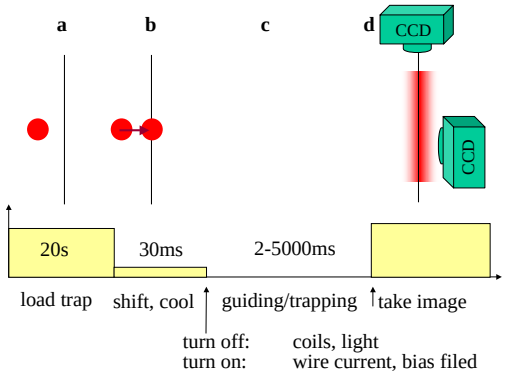

Fig. 4a–d. Steps of the guiding and trapping experiments. **a** Atoms are loaded into the MOT displaced typically 1 mm from the wire. **b** Atoms are then shifted onto the guiding position, the light and MOT fields are turned off and the guiding/trapping fields are turned on. **c** With the light off and the guiding fields on atoms move in the designed potentials. **d** After a given guiding/trapping time, the spatial distribution of the atoms is measured by imaging the fluorescence from optical molasses using the CCD cameras

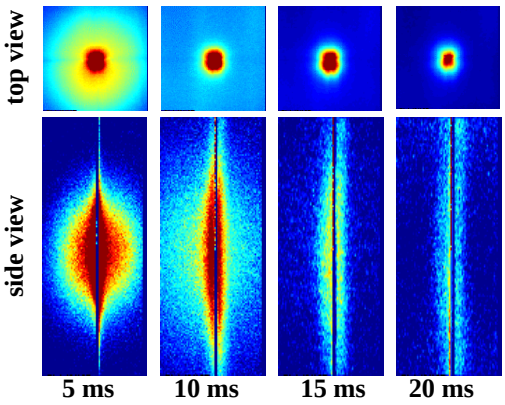

Fig. 5. Guiding of atoms along a current-carrying wire in their *strong-field-seeking* state (Kepler guide). Pictures of the atomic clouds taken from above and from the side are shown. For times shorter than 15 ms the expanding cloud of untrapped atoms is also visible. The location of the wire is indicated by a line (dot). The pictures show a 2-cm-long section of the wire that is illuminated by the laser beams

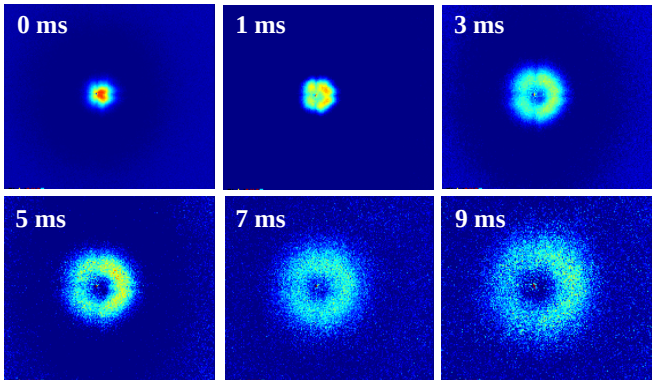

Fig. 6. Atomic distribution after free expansion of 1 to 9 ms for atoms that have been guided in Kepler orbits around the wire. The expanded cloud is doughnut-shaped due to the orbital motion of the atoms around the wire. In the pictures for 1 and 3 ms, cross-shaped shadows in the atomic cloud can be seen that are cast into the laser beams by the wire

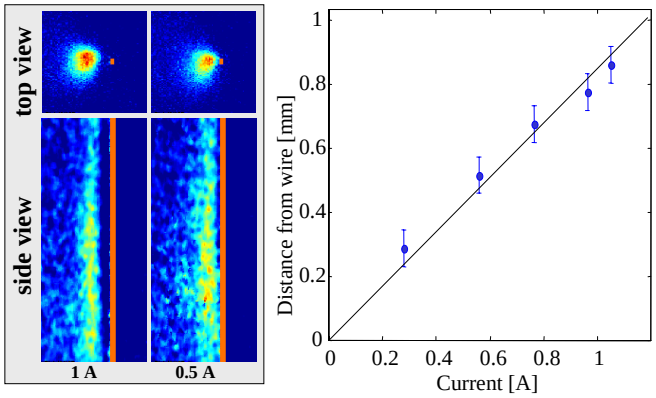

Fig. 7. With an additional bias field atoms in the *weak-field-seeking* state are guided *on the side* of the wire (20 ms guiding time). Choosing different currents through the wire (0.5 A and 1 A for the left graph) the distance of the side trap from the wire can be controlled. Decreasing the current brings the 2-D trap closer to the wire and consequently makes it smaller and steeper

microscopic trapping and guiding potentials (see Fig. 2b) is explained by the fact that the magnetic field $\boldsymbol{B}$ itself has vector character but the effective potential an atom sees in the adiabatic approximation is proportional to the modulus of the magnetic field $|B|$. One has therefore an additional degree of freedom, the direction of an added field, to modify the trapping potential.

Experiment. To load the atoms into the side guide we proceed exactly as for the Kepler guide, the difference being that along with the wire current (typically 1 A) we also switch on a bias field of 2 Gauss. The pictures in Fig. 7 show atoms that are bound to the side guide after 20 ms of guiding time. In the given examples two different currents (1 A and 0.5 A) were sent through the wire. The distance of the guided atoms from the wire changes clearly with the current flowing through the wire.

The side guide has interesting properties: For a given homogeneous bias field $\boldsymbol{B}_\mathrm{b}$ the trap depth is determined by the *magnitude* of the bias field, while the trap size and its distance from the wire are given by the current I through the wire. At the center of the trap the magnetic field gradient scales with B_b^2/I. Here the paradoxical situation arises that the trap gets steeper for *decreasing* current in the wire. Having the trap depth fixed by the bias field, a compression of the trap can be accomplished by *decreasing* the current in the wire and an expansion by *increasing* the current in the wire.

The right hand side of Fig. 7 shows an experimental study of this dependence. The position of the trap was measured from fits to the atomic distribution in the CCD images. The predicted linear dependence of the trap position on the wire current (distance $r_\mathrm{s} \propto I/B_\mathrm{b}$) is confirmed. Pushing the trap closer to the wire while keeping its depth constant results in making the trap steeper with decreasing current. The smallest and steepest trap achievable by a fixed bias field is thereby given by the requirement that the potential minimum lies outside the wire. A simple calculation shows that one can easily have traps with gradients of over 1000 Gauss/cm with a moderate current of about 100 mA and an offset field of 5 Gauss. The guide would be then located 40 μm from the wire.

In the experiments shown in Fig. 7 about 5% of the atoms from an unpolarized atomic sample are loaded into the side guide, in good agreement with Monte Carlo calculations. By

optically pumping the atoms and better 'mode-matching' the temperature and the size of the cloud, one can obtain loading rates of 80% and higher for the side guide.

In contrast to the Kepler guide, the velocity distribution in the side guide is Gaussian as expected for a trapped thermal gas.

1.4 3-dimensional wire traps

The principles shown above can easily be extended in order to build three-dimensional atom traps, simply by adding 'endcaps' to the wire guide (Fig. 8a). The resulting trapping potential is very similar to a Joffe–Pritchard trap. Having the current in the endcap-wires flowing in the same direction automatically removes the zero in the magnetic field, and the trap (if not too elongated) is stable against Majorana transitions. Producing the magnetic trapping potentials with wires and a homogeneous bias field has the advantage that, compared to common magnetic trap designs, only very small currents are necessary to produce very high gradients. With magnetic traps built in a geometry like that shown in Fig. 8a, it is easy to reach and even exceed trap parameters used in recent Bose–Einstein condensation experiments [5] with only a few Watt of power consumption. Wire traps might therefore be an alternative conventional magnetic trap designs where thick coils and high currents have to be used to produce high gradients (see also Sect. 3).

Other three-dimensional wire traps can be created by adding bias fields of special symmetries to the field of a current-carrying wire. One such example is shown in Fig. 8b: A current-carrying wire is used to "plug" the central zero-field "hole" of a 3-D magnetic quadrupole trap. In this way the 3-D quadrupole trap transforms into a torus-shaped magnetic trap. We expect traps of this kind to be useful for experiments studying circular flow and vortices in Bose-Einstein condensates.

We realized such magnetic traps in our recent experiments shown in Fig. 9. We built a Joffe–Pritchard-like trap by using a Z-shaped wire (Fig. 9a), the upper and lower bar of the Z taking over the roles of the two endcap wires in Fig. 8a. We easily obtained field gradients in access of 500 G/cm with only a few Watt of power consumption [24]. In a different experiment we realized a plugged quadrupole trap (Fig. 9b): in our setup the wire going through the center of the quadrupole trap was orthogonal to the symmetry axis of the magnetic quadrupole field. With the rotational symmetry of the trap-

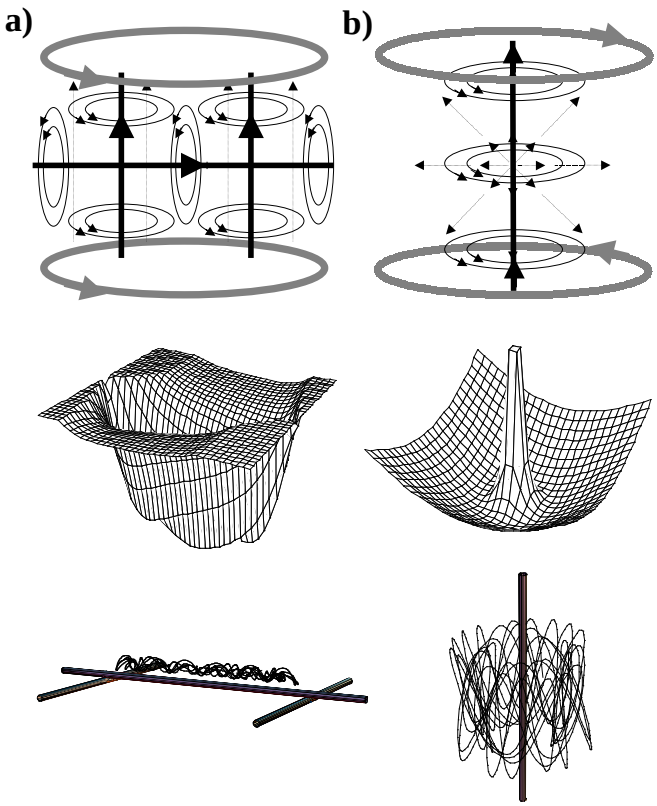

Fig. 8a,b. Two examples of configurations for a three dimensional wire trap. **a** A side guide with endcaps resulting in a magnetic field configuration similar to a Joffe–Pritchard trap. Having the current in the endcaps flowing in the same direction automatically removes the zero in the magnetic field, and the trap is stable against Majorana transitions. **b** A doughnut-shaped trap is created by placing a current-carrying wire in the center of a 3-D quadrupole trap. The field of the wire closes the spin flip leak of the quadrupole trap

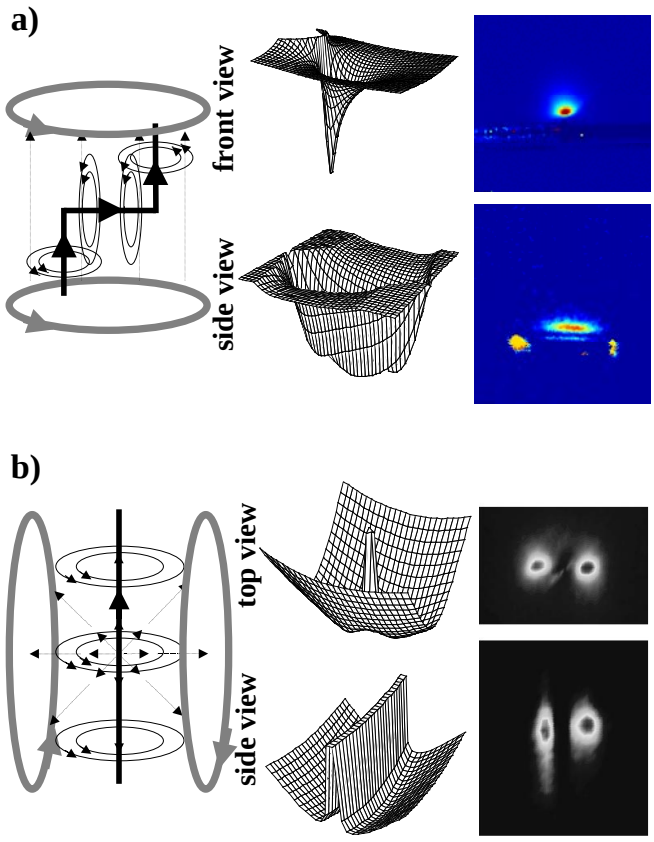

Fig. 9a,b. Experiments showing the trapping of atoms in 3-dimensional wire traps. **a** Atoms are trapped in a Joffe–Pritchard-style trap created by a Z-shaped wire and a bias field. The sideview picture shows the atoms in a cigar shaped cloud hovering above the illuminated wire. The two light spots left and right are reflections off the bend wires that run along the direction of view. **b** Atoms are trapped in a combination of a magnetic quadrupole trap and the magnetic field of the wire. The wire direction is orthogonal to the symmetry axis of the magnetic quadrupole field. The resulting potential is therefore *not* a symmetric ring, but exhibits two additional minima. In each case the configurations, the trapping potentials, and the fluorescence images of the trapped atoms are shown

ping field broken, the resulting ring trap exhibits two additional minima. The lithium atoms were mainly trapped in these minima [13, 14].

A similar wire-based small magnetic trap was realized recently by Fortagh et al. [25]. Even more elaborate designs for traps than the ones described here can be envisioned. See for example J.D. Weinstein, K. Libbrecht [26], or the recent proposal by Hänsch [29]. Similarly one can design guides and traps by replacing the current-carrying wires by adequately shaped permanent magnetic structures. Using the field of a magnetic tip modified by a bias field allows the creation of steep microscopic traps as recently demonstrated by V. Vuletic et al. [27] and magnetic edges could be used to build guides [28].

1.5 Loading into the atom guides

In our experiments we used a pulsed source, the MOT, for loading the guides. Continuous loading can also be achieved by choosing a different experimental setup from the one just described. We here briefly discuss two possibilities:

1. Continuous loading can be done by using a (slow) atomic beam that is directed along the current-carrying wire: for example, by sharply bending the current-carrying wire, an "entrance facet" of the guide is created. An atomic beam aimed directly at this entrance will enter non-adiabatically into the guiding potential. This loading method was used in the first guiding experiment in 1992 [9, 10] and is also similar to the one used for loading atoms into hollow optical fibers [30].
2. A second possibility is loading the guides quasi-continuously: atoms from a 3-D magnetic trap, that serves as a reservoir of cold atoms, leak out of the magnetic trap into the guide. This is accomplished by using a magnetic trap configuration as displayed in Fig. 8a and lowering one of the endcaps. Such a scheme can especially be favorable for loading a BEC into the atom guide (see also Sect. 3).

2 An atom and a charged wire

We now consider the interaction of a neutral polarizable atom (polarizability α) with a charged wire (line charge q) inside a cylindrical ground plate [7, 8, 10, 31] (see also Fig. 1b). The electric field of the charged wire polarizes the atom creating a small electric dipole. The electric field gradient then results in an attractive force between the polarized atom and the wire. The *attractive* interaction potential (in cylindrical coordinates) is given by:

$$V_{\rm pol}(r) = -\frac{1}{2}\alpha E^2(r) = -\left(\frac{1}{2\pi\epsilon_0}\right)^2 \frac{2\alpha\, q^2}{r^2}\,. \tag{2}$$

It has exactly the same radial form ($1/r^2$) as the centripetal potential barrier ($V_L = L_z^2/2Mr^2$) created by angular momentum L_z. V_L is *repulsive*. The total Hamiltonian for the radial motion is

$$H = \frac{p_r^2}{2\,M} + \frac{L_z^2}{2\,M\,r^2} - \left(\frac{1}{2\pi\epsilon_0}\right)^2 \frac{2\alpha\, q^2}{r^2} = \frac{p_r^2}{2M} + \frac{L_z^2 - L_{\rm crit}^2}{2Mr^2}\,, \tag{3}$$

where $L_{\rm crit} = \sqrt{M\,\alpha}\,2q/2\pi\epsilon_0$ is the critical angular momentum characteristic for the strength of the electric interaction. There exists no stable orbit for the atom around the wire. Depending on whether L_z is greater or smaller than $L_{\rm crit}$ the atom either falls into the center and hits the wire ($|L_z| < L_{\rm crit}$) or escapes from the wire towards infinity ($|L_z| > L_{\rm crit}$).

2.1 Scattering experiments probing the $1/r^2$ singularity

Even though stable trapping with a plain charged wire is not possible, the interaction potential between a neutral atom and a line charge is interesting in itself. It is an experimentally realizable example of a singular $1/r^2$ potential [7, 8] that so far was only discussed in textbooks. The $1/r^2$ potential is special among all singular potentials because it lies on the border between $1/r^n$ potentials where the radial motion can be stabilized by angular momentum ($n < 2$) and those where this is not possible ($n > 2$). The $1/r^2$ singularity has a very characteristic way of capturing particles from the surrounding phase space. This can be experimentally demonstrated by measuring the "absorption" cross section for cold atoms impinging on a charged wire [8].

To illustrate this let us consider a monochromatic atomic beam with momentum $p = \hbar k$ approaching an infinitely thin charged wire. The atoms are attracted towards the wire and all those with angular momentum $|L_z| < L_{\rm crit}$ will spiral onto the wire where they are absorbed. Classically the absorption cross section of the charged wire is then simply given by the largest impact parameter $b_{\rm max}$ for which atoms hit the wire ($b_{\rm max} = L_{\rm crit}/p$). The critical angular momentum $L_{\rm crit}$

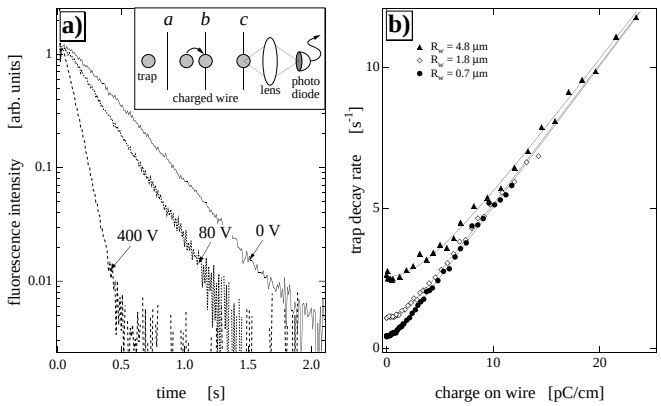

Fig. 10. a When moved onto the wire the atom trap decays exponentially, as can be seen by monitoring the atomic fluorescence signal. Charging the wire (100 V ≈ 6.4 pC/cm) creates an attractive $1/r^2$ potential and enhances the decay rate. *Insert:* Steps a, b, and c are discussed in the text.
b Dependence of the trap decay rates on the wire charge for wires of different thickness. The decay rate for uncharged wires is proportional to their actual diameters. For increasing charges the absorption rate becomes a linear function of the charge, a characteristics of the $1/r^2$ singularity. The slope is independent of the wire diameter

Table 2. Typical parameters for the interaction of neutral atoms (polarizability α) [32] with a charged wire. Δq is the charge that has to be added to the wire to capture one additional partial wave. This charge corresponds to a voltage ΔU applied to a 1-μm-diameter wire surrounded by a grounded cylinder with a diameter of 1 cm

Atom	Polarizability α $\text{Å}^3 4\pi\epsilon_0$	Δq pC/cm	ΔU V
He	0.205	15	2.5
Li	24.3	1.04	0.17
Na	24.1	0.58	0.10
Rb	47.3	0.21	0.035

grows linearly with the applied voltage (charge) on the wire and so does the classical absorption cross section. For wires with a nonzero diameter the cross section at zero charge has a positive offset which corresponds to the thickness of the wire.

Figure 10 shows our recent experiments studying the absorption cross section of cold Li atoms from three different charged wires with 0.7 μm, 1.8 μm, and 4.8 μm radius [8]. After loading and cooling the atoms in a MOT, the trap was shifted onto the charged wire and the trapping laser light intensity turned down to very low light levels, just enough to hold the atoms. The decay of the trap fluorescence (Fig. 10a) is then characteristic for the absorption cross section of the charged wire and the dependence of the trap decay rates as a function of the voltage on the wire shows the characteristics of the $1/r^2$ singularity (Fig. 10b). The trap decay rate increases linearly with the applied charge (voltage) and, for sufficiently high charges, is independent of the wire diameter and atomic velocity. Measuring additionally the size and temperature of the atomic cloud allows the absorption cross section to be calculated from the measured decay rates. For the thick wire ($R_w = 4.8\,\mu\text{m}$) it agrees to within 5% of the predicted cross sections calculated from the published values of the polarizability $\alpha_{\text{Li}} = 24.3\,[\text{Å}^3]$ [32].

Even though the smallest wires had radii R_w that were on the order of the wavelength of light (about 4–5 times larger than the deBroglie wavelength, $\lambda = 2\pi/k$, of the cold Li atoms), the above experiments are still in a classical regime. The characteristic scale here is given by the dimensionless quantity kR_w which corresponds to the angular momentum of a atom with impact parameter $b = R_w$. In our present experiments we find $kR_w \approx 30$ or larger. Using thinner wires and colder atoms (as obtained for example from a BEC) one can easily reach a regime where $kR_w \approx 0.1$ and study the $1/r^2$ singularity in the quantum limit.

For $kR_w < 1$ we have to consider that the angular momentum is quantized and the absorption cross section will not simply increase linearly but rather in distinct steps [7]. Successive partial waves will be absorbed as the charge on the wire is increased. Table 2 gives typical experimental parameters for absorbing single atomic partial waves. This is illustrated by the more detailed quantum calculation of the absorption cross section for several wire diameters as shown in Fig. 11. For thin wires ($kR_w < 1$) the 'quantization' of the absorption cross section is clearly visible but for increasing wire diameters the steps gradually smear out. This can be understood in two ways. One contribution is due to reflection at the centrifugal potential: partial waves that should be absorbed as discussed previously can partially escape. The other contribution is due to tunneling of partial waves through the centrifugal barrier to the absorbing surface of the wire.

2.2 Van der Waals interaction

Working with cold atoms in the direct vicinity of the wire, interactions between the atom and the surface become important. Indeed, in our absorption experiments the Van der Waals interaction represents another attractive force besides the $1/r^2$ potential of the charged wire. This leads to an increase of the wire's cross section for absorbing the lithium atoms: The *effective* diameter of the wire will appear larger than the geometrical cross section. Simple calculations show that for cold Li atoms the effective radius of a wire can be increased by as much as 300 nm, which is significant for thin wires ($r < 1\,\mu\text{m}$).

We were able to observe this effect recently in our absorption experiments. For example for 200-μK cold Li atoms (0.5 m/s velocity) we found an increase in the apparent size of a 1.8-μm-radius gold-coated quartz fiber in the range of 0.2 μm. Our charged wire absorption experiments are sensitive enough that quantitative measurements of the interactions between cold atoms and thin wires ($r < 1\,\mu\text{m}$) should be possible.

2.3 Guiding atoms with a charged optical fiber

As discussed above trapping in the attractive $1/r^2$ potential is not possible. To obtain stable orbits for motion of an atom

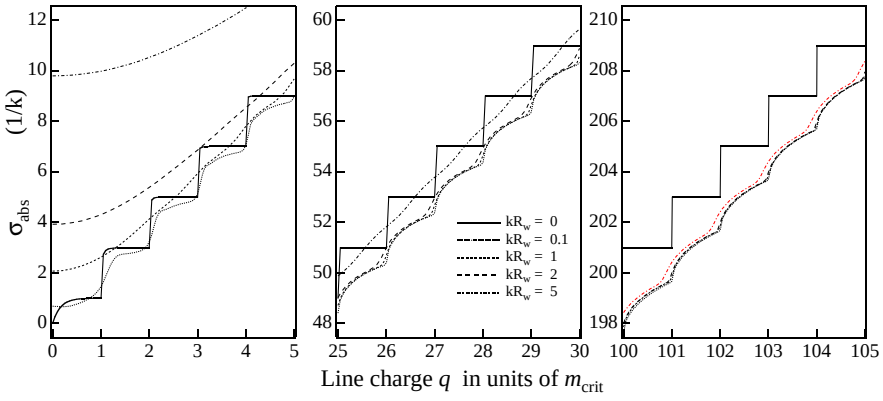

Fig. 11. Theoretical absorption cross section for a charged wire. The calculations are made for several different relative thicknesses (kR_w) of the wire $\hbar\, m_{\text{crit}} = L_{\text{crit}}$

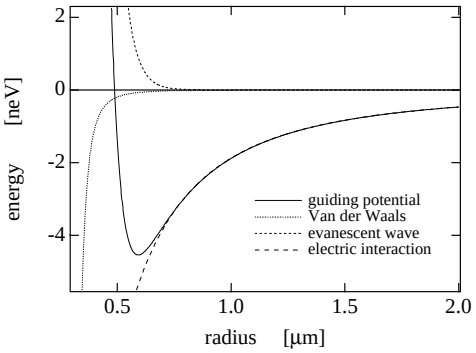

Fig. 12. Typical radial potential for a neutral Li atom trapped around a charged (5 V) optical quartz fiber (diameter 0.5 μm) with 1 mW light and a detuning of $\Delta/\Gamma = 3 \times 10^5$. The attractive potential ($1/r^2$) is created by the interaction of the induced dipole moment in the electric field of the charged fiber. The repulsion is due to the evanescent wave from blue-detuned light propagating in the fiber. Close to the wire surface the Van der Waals interaction becomes important

around a line charge, the atom must be prevented from hitting the wire by a strong repulsive potential near the surface of the wire. Such a strong repulsion can be obtained by the exponential light shift potential of an evanescent wave that is blue-detuned from an atomic resonance. This can be realized by replacing the wire by a charged *optical fiber* with the cladding removed and the blue-detuned light propagating in the fiber [33]. The fiber itself has to be conducting or coated with a thin ($\ll \lambda$) conducting layer to allow for uniform charging of the fiber. For the simple case of a TE_{01} mode propagating in the fiber the ac-Stark shift potential is independent of the polar angle and the combined guiding potential is then given by:

$$V_{\text{guid}}(r) = A\, K_0^2(Br) - \left(\frac{1}{2\pi\epsilon_0}\right)^2 \frac{2\alpha q^2}{r^2}\,, \tag{4}$$

where A and B are constants that depend on specifics of the optical fiber (n, R_w, ...) as well as light power, wavelength, and atomic properties [33]. K_0 is the modified Bessel function of the second kind. Figure 12 shows a typical example of such a potential. Cold atoms are bound in radial direction by the effective potential but free along the z direction, the direction of the charged optical fiber.

Furthermore, as we will show in the next section, in order to turn a charged wire into an atom guide the cylindrical geometry can be abandoned. An atom guide can also be formed by mounting the charged wire into a planar atom mirror.

3 Mesoscopic atom optics

We will now investigate how the basic concepts demonstrated in the above experiments can be used to build mesoscopic systems for neutral atoms [6]. To achieve this the guiding and trapping potentials have to be "microscopic", i.e. their transverse dimension has to be similar to the deBroglie wavelength of the atoms. Because the trap frequencies will then be high compared to the atomic temperature, only a few transverse guide modes will be excited. With a BEC, single-mode propagation should then be possible and the miniaturized atom guide can be considered a coherent wave guide for neutral atoms.

Steep (microscopic) potentials can be realized using very small material structures (for example thin filaments). The extreme fragility of such structures would demand mounting them on a surface. Once mounted even thin wires can sustain strong electric forces and support sizable currents because they can be cooled efficiently [34].

Mounting the charged and/or current carrying structures on a surface restricts the useful potentials to designs where the atoms are confined in traps or guides hovering above the surface. However, one has the advantage that nanofabrication technologies can be used in order to realize complex atom optical circuits on the smallest scale. The question arises how these atom optical circuits on a surface can be loaded with cold atoms. A possible solution could be to load cold atoms (or a BEC) into a free-standing wire-guide [9, 12], as demonstrated in our experiments described in Sect. 1.3 which then transports the atoms to the surface-mounted mesoscopic devices.

Because of the similarity to quantum electronics [1] we will call structures that provide one dimensional confinement, i.e. atoms are allowed to move freely along the surface, a *quantum well*. Structures with two-dimensional confinement, i.e. a microscopic atom guide, we will call a *quantum wire*; three-dimensional confinement we will call a *quantum dot*.

We will now briefly discuss some options for matter-wave optics above surfaces for magnetic and electrical potentials.

3.1 Current-carrying structures, the magnetic interaction

The guides and traps realized by the magnetic field of current-carrying wires modified by a bias field [12] (see Sect. 1.3

Table 3. Typical potential parameters for quantum wires created by *(top)* a thin current-carrying wire mounted on a surface with an added bias field, and *(bottom)* a charged wire mounted on a magnetic atom mirror. The directions x and y refer to orthogonal and parallel to the surface. z is along the wire. The electric quantum wire potential is asymmetric and ground-state parameters are given for x and y. In the case of the magnetic quantum wire the harmonic potential minimum is symmetric. See also figure Fig. 13

Quantum wires based on current-carrying wires							
Atom	Wire current	B_{bias}		Potential		Ground state	
		y	z	depth	distance	freq.	size
	mA	G	G	neV	μm	kHz	μm
Li	1	1	1	6	2	22	0.25
Li	10	10	5	29	2	100	0.12
Rb	1	1	0.5	6	2	9	0.11
Rb	10	10	2	29	2	45	0.051

Charged wires mounted on a magnetic mirror $U_m = 6.4\,\mu\text{eV}$ ($B_0 = 1100$ G) $\kappa = 1.5\,\mu\text{m}$							
Atom	Wire charge	Potential		Ground state properties			
		depth	distance	frequency in kHz		size in μm	
	pC	neV	μm	x	y	x	y
Li	5.2	-3.3	13	10	4.3	0.38	0.58
Li	16	-76	7.2	56	43	0.16	0.18
Rb	4.3	-4.8	12.5	3.5	1.6	0.18	0.28
Rb	11	-65	7.5	15	11	0.09	0.11

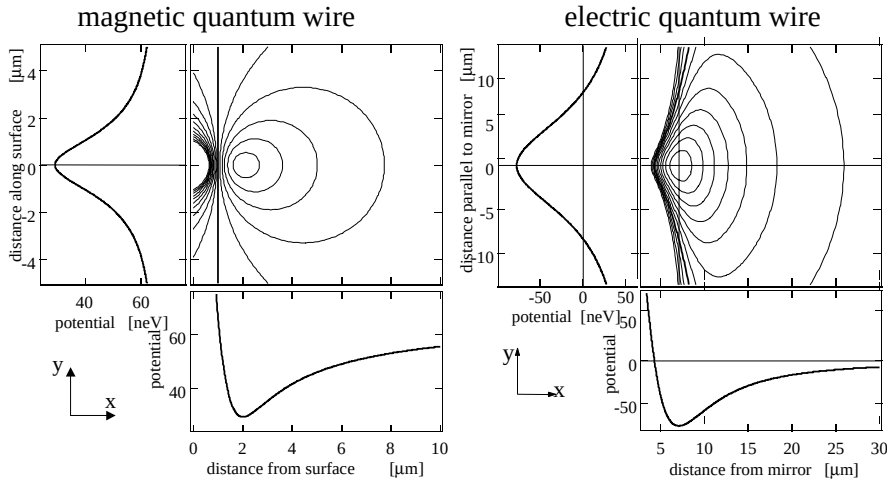

Fig. 13. Typical potentials for quantum wires created by *(left)* a thin current-carrying wire (10 mA) mounted on a surface with an added bias field ($B_x = 10$ G, $B_z = 5$ G), and *(right)* a charged wire (16 pC/cm) mounted on an atom mirror. The potentials shown are for the parameters given in Table 3 for Li atoms

and 1.4) have favorable scaling properties and can easily be miniaturized. Absorption of atoms at the surface is prevented by locating the guiding/trapping potential above the surface which can be achieved using the *side guide* [12] (see also the proposal [29]), that is by adding a homogeneous bias field parallel to the surface and (almost) orthogonal to the wire. An additional component of the bias field in the direction of the wire removes the zero in the magnetic field and makes the motion in the guide/trap be stable against spin flip transitions.

Examples of typical guiding parameters are given in Table 3 and on the left side of Fig. 13. For example gradients exceeding about 10 000 Gauss/cm and curvatures larger then 10^8 G/cm^2 leading for Li atoms to trap frequencies up to 100 kHz can be achieved with a moderate current of about 10 mA and a magnetic offset field B_b of 10 Gauss. The guided atoms are then located a few μm above the surface.

Combining two wires one can easily imagine building a beam splitter or even an interferometer. Atoms can be directed by switching the currents, or can be stopped and released by additional wires, similar to the endcaps of the Joffe–Pritchard trap described in Sect. 1.4.

We recently performed experiments on such a beam splitter, although not yet in the quantum regime. The beamsplitter consisted of two free-standing wires that were combined to form a 'Y'. By controlling the current through the arms of the Y-shaped wire we can send cold Li atoms along either of the two arms of the Y and thus demonstrate a novel atom switch. If current is send through both arms the atom beam is split into two [14] (Fig. 14).

A similar device can also be constructed that does not split and recombine atom beams but traps. For example let us consider two wire traps (as in Sect. 1.4) that are placed next to each other in a parallel way. Depending on the magnitude of the magnetic bias field the two traps merge together or separate as depicted in Fig. 15.

These design principles for mesoscopic magnetic potentials are not restricted to current-carrying wires. Similar designs should also be possible using nanofabricated permanent magnetic structures [28] (see also Sect. 1.4).

3.2 Charged structures, the electric interaction

Similarly, as described in [6], a large variety of mesoscopic potentials can be created by placing a charged nanostructure on an atomic mirror [35, 36] (see Fig. 13). The electric field of the charged structure creates an attractive potential (2). The repulsive potential of the atomic mirror prevents the atoms from reaching the surface. The combination of both creates vertical and transverse confinement.

For example by mounting a charged wire on an atomic mirror one can build a tube-like potential created by an interplay between the attractive potential ($1/r^2$) created by the charged wire and the repulsion of the atomic mirror

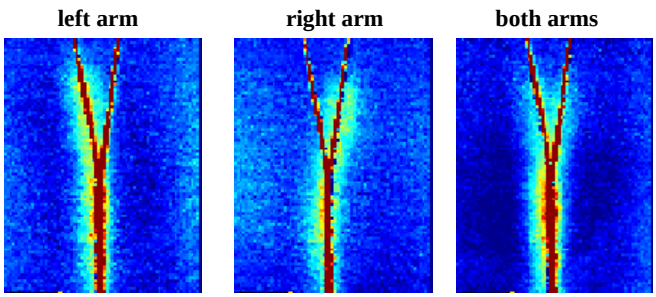

Fig. 14. Beam splitter for guided atoms (Kepler guide) using a Y-shaped current carrying wire. By controlling the current through the arms of the Y we can send cold Li atoms along either arms of the Y or split the beam into two

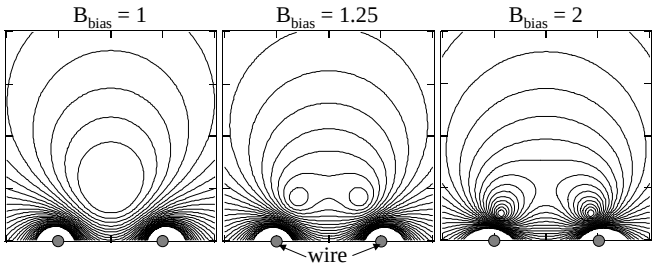

Fig. 15. Potential for two wire traps close together. By changing the bias field we can split and recombine the two traps. *(left)* Applying a weak (compared to the current in the wire) bias field results in one trap. *(right)* Applying a strong (compared to the current in the wire) bias field gives two separate traps close to the wires

(Fig. 13) [6]:

$$V(\boldsymbol{x}) = V_0 \exp(-\kappa_m z) - \left(\frac{1}{2\pi\epsilon_0}\right)^2 \frac{2\alpha q^2}{\rho^2}\,, \tag{5}$$

where z is the distance above the mirror surface, $\rho = \sqrt{x^2+y^2}$ is the distance from the wire (in cylindrical coordinates) and $1/\kappa_m$ is the characteristic length scale of the repulsive interaction[2].

Typical parameters for such guides formed by a magnetic mirrors and a charged wire are shown in Table 3 and on the right side of Fig. 13. They can be very similar to the magnetic quantum wires discussed above. Using the mirror parameters from T.M. Roach et al. [36] one can easily achieve deep and narrow guides with transverse level spacings in the kHz range, for both light (Li) and heavy (Rb) atoms. An estimate of the tunneling probability to the mirror surface gives lifetimes of atoms in these quantum wires much longer than 1000 s. Such a mesoscopic potential can be viewed as a *quantum wire* for neutral atoms.

Similarly one can build *quantum dots* (small microscopic traps) by mounting charged points (attractive $1/r^4$ interaction) on the atomic mirror [6]:

$$V(\boldsymbol{x}) = V_0 \exp(-\kappa_m z) - \left(\frac{1}{2\pi\epsilon_0}\right)^2 \frac{2\alpha q^2}{r^4}\,, \tag{6}$$

where $r = \sqrt{x^2+y^2+z^2}$ is the distance from the charged point.

3.3 Outlook: creating mesoscopic quantum networks

These mesoscopic potentials and guides created by mounting nanofabricated charged and current-carrying structures on a surface or an atomic mirror have many advantages which make them promising for future applications. This is partly due to the robustness and versatility of the electrical and magnetic potentials which allows many degrees of freedom in manipulating atomic wavefunctions.

The electric and the magnetic interactions can be combined to tailor the potentials. For example additional supplementary electrodes located close to a guiding wire can be used to modify the guiding potential on demand. One can easily imagine designing switches, gates, modulators, etc. for guided atoms.

Similarly having the atoms trapped or guided, well localized near the surface, will allow the integration of atom optics and light optics. Waveguides for light can be fabricated onto the surface. These can be used to address or detect individual neutral atoms in the quantum wires or quantum dots. The atoms can be shifted in and out of resonance by applying additional fields using supplementary electrodes. Such integrated optics devices for atom light manipulation might be used to build quantum registers for quantum communication and quantum computation.

[2] For an evanescent wave mirror the length scale is given by: $\kappa = 2k\sqrt{n^2\sin^2\theta_i - 1}$ (k is the wave vector of the light, n is the refractive index of the glass and θ_i the incident angle of the laser beam). For a magnetic mirror [36] the characteristic length scale is given by $\kappa = 2\pi/d$ where d is the size of the magnetic domains forming the mirror

Coupling between atoms in different channels of a network can be achieved using the atom–atom interaction, for example by sending them on a beam splitter [6]. For example the effect of atom–atom interaction on quantum statistics in a waveguide beam splitter was recently discussed in [37]. Because it should be possible to entangle atoms by their mutual interactions one should be able to construct quantum gates using atoms confined to quantum dots (see for example [38, 39]) or propagating in these quantum wires.

This leaves the question of how to load these mesoscopic guides and traps. The simplest solution would be to create a BEC as a reservoir of cold atoms directly in a surface-mounted Z-trap as discussed in Sect. 1.4 and load the atoms from there using surface-mounted atom guides. A different possibility would be to load cold atoms, possibly a BEC into a free-standing wire-guide (Sect. 1.3) which then transports the atoms into the mesoscopic devices.

4 Conclusion

In the early days of atom optics it was desirable to separate atoms as far as possible from material objects in order to obtain pure and isolated quantum systems. Today cooling and trapping techniques are so well developed that there is now an interest in bringing the atoms close to material macroscopic objects where the proximity of the atoms to the object allows for the design of new controllable potentials and atom optical elements. In our experiments over the last five years, some of them reported here, we have shown that such traps and guides are feasible. Using these techniques miniaturization of atom optical elements and later on integration of many atom optical elements into one single quantum circuit should be possible in the near future.

Nanofabricated atom optical elements on a surface will allow us to combine the best of two worlds: the tools of quantum optics and the long coherence times and very high precision of neutral atom manipulation, with the vast technology of integrated optical and electronic elements. Together these techniques will be integrated in one single *atom chip* which can be produced using nanofabrication technology. We expect this new technology to bring a very significant advance in our ability to control and manipulate quantum systems. The latter will enable new fundamental experiments in quantum optics and quantum information processing [39] and allow the development of novel devices using neutral atoms.

Acknowledgements. We thank B. Hessmo, A. Haase, P. Krüger, and R. Folman for help in the final stages of the experiments and A. Zeilinger for his generous support throughout the work. This work was supported by the Austrian Science Foundation (FWF), project S065-05 and SFB F15-07, the Jubiläums Fonds der Österreichischen Nationalbank, project 6400, and by the European Union, contract Nr. TMRX-CT96-0002.

References

1. See for example: *Quantum Coherence in Mesoscopic Systems*, ed. by B. Kramer, NATO ASI Series B: Phys. Vol. **254**, Plenum (1991)
2. See for example: B.E.A. Saleh, M.C. Teich: *Fundamentals of Photonics* (J. Wiley, New York 1991)
3. For an overview see: C.S. Adams, M. Sigel, J. Mlynek: Phys. Rep. **240**, 143 (1994); *Atom Interferometry*, ed. by P. Berman (Academic Press, New York 1997) and references therein

4. A good overview of laser cooling is given in: E. Arimondo, W.D. Phillips, F. Strumia (Eds.): *Laser Manipulation of Atoms and Ions* (North Holland, Amsterdam 1992); S. Chu: Rev. Mod. Phys. **70**, 685 (1998); C. Cohen-Tannoudji: Rev. Mod. Phys. **70**, 707 (1998); W.D. Phillips: Rev. Mod. Phys. **70**, 721 (1998).
5. M.H. Anderson et al.: Science **269**, 198 (1995); K.B. Davis et al.: Phys. Rev. Lett. **75**, 3969 (1995); M.-O. Mewes et al.: Phys. Rev. Lett. **77**, 988 (1996); C.C. Bradley, C.A. Sacket, R.G. Hulet: Phys. Rev. Lett. **78**, 985 (1997); see also C.C. Bradley et al.: Phys. Rev. Lett. **75**, 1678 (1995). For a complete list of references see the BEC Home-Page http://amo.phy.gasou.edu/bec.html and the cond-mat Los Alamos archive http://xxx.lanl.gov/
6. J. Schmiedmayer: Habilitationsschrift, Universität Innsbruck (1996); J. Denschlag, J. Schmiedmayer: In Proceedings of the International Quantum Coherence Conference, Boston (1997) (World Scientific, Singapore); J. Schmiedmayer: Eur. Phys. J. D **4**, 57 (1998)
7. J. Denschlag, J. Schmiedmayer: Europhys. Lett. **38**, 405 (1997)
8. J. Denschlag, G. Umshaus, J. Schmiedmayer: Phys. Rev. Lett. **81**, 737 (1998)
9. J. Schmiedmayer: In XVIII International Conference on Quantum Electronics: Technical Digest, ed. by G. Magerl (Technische Universität Wien, Vienna 1992), Series 1992, Vol. 9, p. 284 (1992); J. Schmiedmayer: Phys. Rev. A **52**, R13 (1995)
10. J. Schmiedmayer: Appl. Phys. B **60**, 169 (1995)
11. J. Schmiedmayer and A. Scrinzi: Phys. Rev. A **54**, R2525 (1996); JEOS – Quantum and Semiclassical Optics **8**, 693 (1996)
12. J. Denschlag, D. Cassettari, J. Schmiedmayer: Phys. Rev. Lett. **82**, 2014 (1999)
13. J. Denschlag: PhD thesis, Universität Innsbruck (Sept. 1998)
14. D. Cassettari, A. Chenet, J. Denschlag, S. Schneider, J. Schmiedmayer: EQEC 98, Glasgow (Sept. 1998)
15. A. Shapere, F. Wilczek (Eds.): *Geometric Phases in Physics* (World Scientific, Singapore 1988); Y. Aharonov, A. Stern: *Phys. Rev. Lett.* **69**, 3593 (1992); A. Stern: *Phys. Rev. Lett.* **68**, 1022 (1992)
16. W. Wing: Prog. Quant. Electr. **8**, 181 (1984)
17. The Earnshaw theorem can be generalized to any combination of electric, magnetic and gravitational field, as shown in: W. Ketterle, D. Pritchard: Appl. Phys. B **54**, 403 (1992)
18. V.V. Vladimirskii: Sov. Phys. JETP **12**, 740 (1961)
19. A very similar potential can be realized for small polar molecules with a permanent dipole moment interacting with the electric field of a charged wire. S.K. Sekatskii, J. Schmiedmayer: Europhys. Lett. **36**, 407 (1996)
20. G.P. Pron'kov, Y.G. Stroganov: Zh. Eksp. Teor. Fiz. **72**, 2048 (1977) [Sov. Phys. JETP **45**, 1075 (1977)]
21. R. Blümel, K. Dietrich: Phys. Lett. A **139**, 236 (1989); Phys. Rev. A **43**, 22 (1991)
22. A.I. Voronin: Phys. Rev. A **43**, 29 (1991)
23. L. Hau, J. Golovchenko, M. Burns: Phys. Rev. Lett. **74**, 3138 (1995); K. Berg–Sørensen, M. Burns, J. Golovchenko, L. Hau: Phys. Rev. A **53**, 1653 (1996)
24. D. Cassettari et al.: Proceedings of ICOLS99 (1999); D. Cassettari et al.: to be published (1999); for an independent proposal see [29]
25. J. Fortagh et al.: Phys. Rev. Lett. **81**, 5310 (1998)
26. J.D. Weinstein, K. Libbrecht: Phys. Rev. A. **52**, 4004 (1995)
27. V. Vuletic et al.: Phys. Rev. Lett. **80**, 1634 (1998)
28. K. Zimmermann: private communication (1998)
29. J. Reichel et al.: EQEC 98, Glasgow (Sept. 1998)
30. Guiding atoms in hollow optical fibers was proposed by: M.A. Ol'Shanii, Y.B. Ovchinnikov, V.S. Letokhov: Opt. Commun. **98**, 77 (1993); S. Marksteiner, C.M. Savage, P. Zoller, S.L. Rolston: Phys. Rev. A **50**, 2680 (1994); and experimentally demonstrated by: M.J. Renn et al.: Phys. Rev. Lett. **75**, 3253 (1995); H. Ito et al.: Phys. Rev. Lett. **76**, 4500 (1996)
31. L. Hau, M. Burns, J. Golovchenko: Phys. Rev. A **45**, 6468 (1992)
32. T.M. Miller, B. Bederson: Adv. At. Mol. Phys. **13**, 1 (1977)
33. H. Batelaan, R. Abfalterer, S. Wehinger, J. Schmiedmayer: EQEC V Technical Digest 1994 (Amsterdam 1994) p. 13; J. Denschlag, H. Batelaan, J. Schmiedmayer: unpublished
34. M. Drndic et al.: Appl. Phys. Lett. **72**, 2906 (1998)
35. V.I. Balykin, V.S. Lethokov, Y.B. Ovchinnikov, A.I. Sidorov: Phys. Rev. Lett. **60**, 2137 (1988)
36. A.I. Sidorov, R.J. McLean, W.J. Rowlands, D.C. Lau, J.E. Murphy, M. Walkiewicz, G.I. Opat, P. Hannaford: JEOS – Quantum and Semiclassical Optics **8**, 713 (1996); T.M. Roach, H. Abele, M.G. Boshier, H.L. Grossman, K.P. Zetie, E.A. Hinds: Phys. Rev. Lett. **75**, 629 (1995)
37. E. Andersson, M.T. Fontenelle, S. Stenholm: Phys. Rev. A **59**, 3814 (1999)
38. D. Jaksch, H.-J. Briegel, J.I. Cirac, C.W. Gardiner, P. Zoller: Phys. Rev. Lett. **82**, 1975 (1999)
39. T. Calarco, E.A. Hinds, D. Jaksch, J. Schmiedmayer, J.I. Cirac, P. Zoller: quant-ph/9 905 013